Special Conference Edition, November, 2018

http://dx.doi.org/10.4314/bajopas.v11i1.29S

Bayero Journal of Pure and Applied Sciences, 11(1): 178 - 184
ISSN 2006 – 6996

INSIGHT FROM THE STUDY OF ACIDITY AND REACTIVITY OF Cr_2O_3 CATALYST IN PROPANE DEHYDROGENATION: A COMPUTATIONAL APPROACH

***Oyegoke, T.[1], Dabai,F.N.[1], Uzairu, A.[2] and Jibril B.Y.[1]**
[1] Chemical Engineering Department, Ahmadu Bello University, Zaria
[2] Chemistry Department, Ahmadu Bello University, Zaria
*Corresponding Author: Oyegoketoyese@gmail.com, +234-8098679625

ABSTRACT
By converting low-value commodity fuels into high-value products, like polymer precursors, chemical and other intermediates, the dehydrogenation of light paraffin (such as ethane and propane) into olefins, can add significant value to the refining processes that generate propane. In this study, the parameterised method 3 (PM3) approximation of semi-empirical theory was employed to study the acidity and reactivity of chromium (III) oxide catalyst in the dehydrogenation of propane into propylene. Ammonia and pyridine were used computationally as molecular probes for the evaluation of the Lewis acidity of the catalyst sites. The propane adsorption and dissociation activation energies were also evaluated. The study showed that the chromium sites are highly acidic and reactive compared to the oxygen sites. In particular, the study showed that the chromium site is the main active site in the promotion of propane dehydrogenation into propylene, over chromium (III) oxide catalyst.
Keywords: Acidity, Reactivity, Dehydrogenation, Propane, Chromium.

INTRODUCTION

The importance of dehydrogenation of propane into propylene cannot be overemphasized. Propylene is one of the vital building blocks in the petrochemical industries. It is often used as a precursor for the production of important intermediate and products, such as polypropylene, isopropanol, epichlorohydrin, propylene oxide, and acrylonitrile (Budavari, 1996; Ren *et al.,* 2009). Several researchers have look into the challenges encountered in its production such as increase in selectivity to propylene and decrease in catalyst deactivations.

Yan *et al.* (2008) employed the use of Density Functional Theory (DFT) calculation to propose a radical mechanism for propane dehydrogenation over Ga_2O_3 (100) and identified H abstraction by O(2) site as a low energy barrier step. DFT calculations conducted by Ming *et al.* (2012) showed that introduction of Sn into platinum catalyst lowers the energy barrier for propylene desorption and simultaneously increases the activation energy for propylene dehydrogenation, which has a positive effect on the selectivity of propylene production. Lauri and Karolina (2013) also made similar deductions for the use of Pt-Sn catalyst, which results in low coking while weakening the binding of propylene. Timothy (2015) confirmed that PtGa alloy has superior catalytic properties than SnGa alloy, and similar properties to those deduced for Pt-Sn alloy (as reported by Lauri and Karolina (2013)). Stephanie *et al.* (2017) found that increase in hydrogen pressure lowers the coverage of deeply dehydrogenated coke precursors on the surface. Other similar findings have been reported by Biloen *et al.*, (1977); Li *et al.,* (2007); Benco *et al.,* (2011) and Ming *et al.,* (2011).

Supported chromium-oxide is known to be active catalyst in oxidative dehydrogenation of propane. It is not clear whether the chromium- or oxygen-site serve as active site in dehydrogenation on the catalyst. Therefore, in this preliminary study, parameterised method 3 (PM3) approximation of semi-empirical theory was employed to study the acidity and reactivity of chromium (III) oxide catalyst in the dehydrogenation of propane into propylene. Ammonia and pyridine were used computationally as molecular probes for the evaluation of the Lewis acidity of the catalyst sites. The propane adsorption and dissociation activation energies were also evaluated in order to determine the effect of different sites on the catalyst.

Computational Details

The computations for this work were carried out with the standard version of semi-empirical calculation method using Parameterized Model 3 (PM3) basis set in the Spartan 14 software package and ran on a Lenovo Ideapad 110 Notebook (Intel Celeron N3060 Processor and 2.00 GB RAM).

The structures of the catalyst, reactant, transition state and molecular probe structures were built and minimized with the use of molecular mechanics (MMFF) method to remove strain energy. All the molecular mechanics optimized geometries were subjected to PM3 and the semi-empirical calculation method was adopted. The PM3 basis set was employed because literature confirms it to be one of the best for computations that involve transition metals, such as Chromium (Warren and Sean, 2017).

The transition states for each step located were confirmed in terms of vibration analysis, through the presence of the imaginary frequency in the IR spectra and output summary tab. Heat of formation for the reactants, transition states, intermediates and products were all calculated. The Infra-Red spectra, molecular, thermodynamics and physiochemical parameters were evaluated from the computational approach employed, and the activation energy, E_a was calculated using the expression below in equation (1):

$E_a = E_{transition\ state} - E_{reactant}$ (Warren and Sean, 2017) (1)

The adsorption energies, E_{ads} were calculated using equation (2):

$E_{ads} = E_{pq} - E_p - E_q$ (Maldonado and Stashans, 2016) (2)

Where, E_a = activation energy, E_{ads} = adsorption energy, E_p = total energy of adsorbate (p), E_q = total energy of free cluster (q), E_{pq} = total energy of adsorbed cluster (pq).

RESULTS AND DISCUSSION

Geometry Optimization of Catalyst, Molecular Probes, and Propane

The results obtained for the molecular and physiochemical properties from the geometry optimization of the catalyst, probes and propane are presented in Table 1. The table shows the total molecular energy (E), highest occupied molecular orbital (HOMO) energy, lowest unoccupied molecular orbital (LUMO) energy, electron affinity and the band gap. Bendjeddou *et al*. (2016) defined electron affinity as the half of the absolute sum of the HOMO and LUMO energy while band gap is the absolute difference between the HOMO and LUMO energy.

Table 1 shows that ammonia has the highest HOMO energy (-9.7 eV) while chromium (III) oxide (Cr_2O_3), has the lowest HOMO energy (-12.08 eV). This implies that ammonia will find it easier to donate an electron compared to Cr_2O_3. Table 1 also shows that propane (C_3H_8) has the highest LUMO energy (3.71 eV) while Cr_2O_3 has the lowest LUMO energy (-3.93 eV). Again, this implies that the Cr_2O_3 is more likely to accept electrons from ammonia, propane or pyridine since they have lower electron affinity and higher band gaps.

Table 1: Molecular and Physiochemical Properties of Catalyst, Probes and Propane

Label	Description	E HOMO (eV)	E LUMO (eV)	E (eV)	Band Gap (eV)	Electron Affinity (eV)
Cr_2O_3	Catalyst	-12.08	-3.93	6.09	8.15	8.005
C_5H_5N	Probe	-10.1	-0.01	1.32	10.09	5.055
NH_3	Probe	-9.7	3.33	-0.13	13.03	3.185
C_3H_8	Reactant	-11.51	3.71	-1.02	15.22	3.900

The stability of the different geometrical structures for the Cr_2O_3, ammonia, pyridine and propane were evaluated using their respective band gaps shown on Table 1. It has been suggested that the lower the band gap, the less stable the molecule with high reactivity (Bendjeddou *et al.,* 2016). The results in Table 1 show that the Cr_2O_3, which has the least band gap, is less stable than Pyridine, which is less stable than Ammonia, which is less stable than Propane. Thus, Cr_2O_3 is the least stable and most reactive, and propane is the most stable and least reactive, amongst the molecules considered.

Table 1 also shows that the catalyst (Cr_2O_3) has the highest electron affinity (8.005 eV) while ammonia (NH_3) has the lowest electron affinity amongst the molecules considered in this study. This indicates that the catalyst will be highly susceptible to accepting electrons through its Lewis acidic sites, otherwise referred to as the electrophilic site (Fukui, 1982; Bendjeddou *et al.,* 2016).

HOMO and LUMO Electron Density Map

In this study of Fukui frontier molecular orbitals, the HOMO and LUMO electron density maps were employed to identify the possible acidic sites and the mode of interaction of molecules with each other as reported by Gece (2008) and Bendjeddou *et al*. (2016). The model used in representing the molecules is the ball and spoke model for molecular structures (as shown on Table 2).

The LUMO and HOMO electron density maps represented on Table 2 have 8-levels of colours showing different levels of electron density. The blue colour shows the highest density (100 %) while the red shows the least density (0 %) on both maps. This gives an insight into the LUMO and HOMO sites on the different molecules, which denotes the sites for electron-reception and electron-donation respectively.

Table 2: HOMO and LUMO Electron Density Maps of Catalyst, Probes and Propane

Label	Molecular Structure	HOMO Electron Density Map	LOMO Electron Density Map
Cr_2O_3	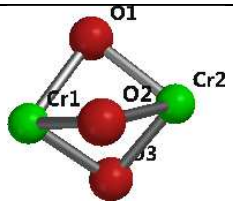	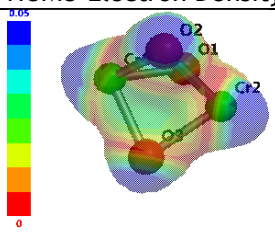	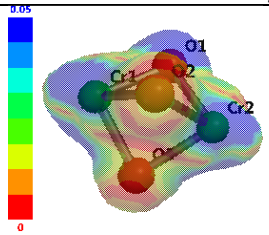
Pyridine	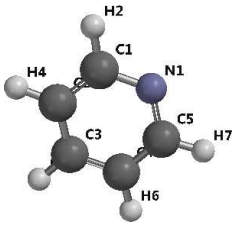	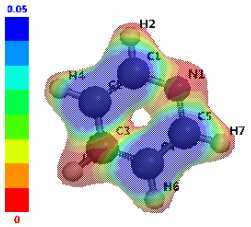	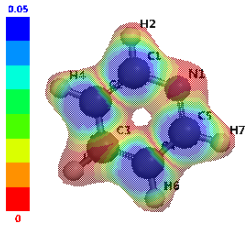
Ammonia	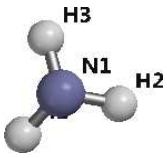	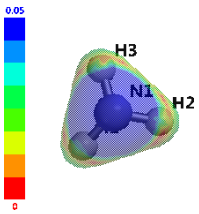	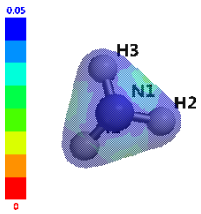
Propane	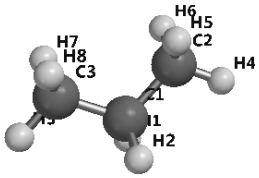	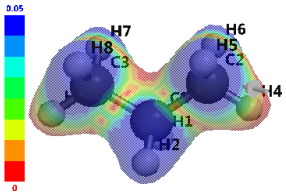	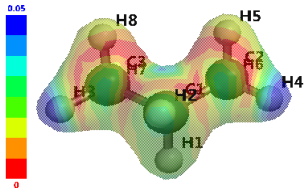

The findings on Cr_2O_3, from the electron density maps (on Table 2), shows that oxygen (O1, O2, O3) atoms are the HOMO sites, while chromium (Cr1, Cr2) and oxygen (O1) atoms are the LUMO sites on the catalyst cluster. For pyridine, the C1, C3, C4 and C5 denotes both the HOMO and LUMO sites, unlike that observed for the Cr_2O_3. The nitrogen (N1) atom was identified to be the HOMO site on ammonia, while the LUMO sites was known to be either of hydrogen or nitrogen atom sites on the structure. For propane, the HOMO sites includes all the hydrogen atoms, except the terminal hydrogen (H4 and H3) atoms, which are the LUMO sites. Based on this study, the O1, Cr1 and Cr2 sites are likely to be the most acidic sites using the LUMO electron density map for Cr_2O_3.

Assessment of Catalyst Sites Acidity using Molecular Probes

The different sites on the chromium (III) oxide were evaluated for acidity using the adsorption energies (E). Pyridine and ammonia were used as molecular probes for the evaluation of catalyst sites acidity (Liu, 2017).

Pyridine Adsorption on Chromium (III) oxide Catalyst: The results obtained from the adsorption of pyridine on Cr_2O_3 catalyst are presented in Table 3, where the adsorption energies (E_{ads}) and bond-lengths (L) are reported. Based on the results presented on Table 3, it can be deduced that the relationship between bond length (L) and adsorption energy (E_{ads}) is a direct relation, which is not in agreement with the 'power law' relationship reported by Gibb *et al.* (1998) or Martins *et al.* (2000) work, which showed that there is no correlation between bond length and bond energy.

The direct relation shown for bond length and adsorption energy was identified to be as a result of the nature of atom pairs involved in the bond held at the different sites (like C1-Cr1, C1-O3, N1-O2, etc.). This means that the higher the adsorption energy, which implies the higher the acidity according to Liu (2017).

Table 3: Pyridine Adsorption Parameters

Probe Site	Catalyst Site	L (A)	|Eads| (eV)
C1	Cr2	2.094	9.170
	Cr1	2.102	9.110
	O1	1.447	7.060
	O2	1.447	7.060
	O3	1.447	7.060
N1	Cr2	1.901	10.420
	Cr1	1.901	10.420
	O1	1.847	7.090
	O2	1.847	7.090
	O3	1.847	7.080

The results on Table 3 shows that the Cr2 and Cr1 sites exhibit similar properties, and the oxygen sites (O1, O2 and O3) also show similar properties. Adsorption of pyridine through the carbon (C1) site, which was as the HOMO site using the electron density map on Table 2, shows the chromium sites exhibit a stronger adsorption bond (9.17 eV) and longer bond length (2.094 A) relative to the oxygen sites (i.e. the other sites) on the catalyst. Similar deductions for bond length and adsorption relations were found for the chromium and oxygen sites, when considering pyridine adsorption through the nitrogen (N1) atom. This implies that the chromium sites are highly acidic relative to the oxygen sites; this agrees with the work of Liu (2017), which states that the adsorption energy of molecular probe is directly proportional to the acidity of the site.

Ammonia Adsorption on Chromium (III) oxide Catalyst: The results obtained from the adsorption of NH_3 on Cr_2O_3 catalyst are shown in Table 4. The results indicate that during the adsorption of ammonia, the oxygen sites display shorter bond-lengths (1.72 A to 1.88 A) compared to the chromium sites with bond-lengths of 1.95 A to 2.48 A. This finding is similar to that observed for the pyridine adsorption earlier discussed.

Table 4: Ammonia Adsorption Parameters

Probe Site	Catalyst Site	L (A)	$\|E_{ads}\|$ (eV)
H1	Cr2	2.477	9.770
	Cr1	2.456	9.770
	O1	1.722	7.470
	O2	1.725	7.480
	O3	1.722	7.480
N1	Cr2	1.952	11.020
	Cr1	1.952	11.020
	O1	1.880	7.580
	O2	1.880	7.570
	O3	1.881	7.580

For both the hydrogen (H1) and nitrogen (N1) sites, the chromium (Cr1 and Cr2) sites were found to have the highest adsorption (absolute) energy of 9.77 eV for hydrogen and 11.02 eV for nitrogen. The oxygen sites showed the lowest adsorption (absolute) energy of 7.47 eV and 7.48 eV for the probe sites of hydrogen, while 7.57 eV and 7.58 eV was obtained for the probe sites of the nitrogen, during the adsorption of ammonia. According to Liu (2017), this implies that oxygen sites can be of low acidity due to the low adsorption energies obtained for the sites unlike that of chromium sites.

It was found that the power law reported in Gibbs *et al.* (1997) and Martin *et al.* (2000) which states that shorter bond are stronger than longer bond, will not be applicable in this case. This was because the bond energies considered in this case have different atom pairs (H1-O3, N1-Cr, etc.) instead of consistent pairs like C-N and C=N or C-C and C=C. This made shorter bond to look weaker and longer bond stronger in this case.

Adsorption Energy Profile across the Catalyst Sites: Adsorption energy profiles (shown in Figure 1) across the catalyst sites for ammonia show that the oxygen sites have the lowest adsorption energy, while the chromium sites showed highest energy. For pyridine, the adsorption energies of the chromium and oxygen sites obeys a similar trend. This confirms that the oxygen sites have the least acidity.

This catalyst site screening approach was in line with procedure reported by Liu (2017) for the theory of acidity and reactivity in catalysis. Liu (2017) established that the relationship between adsorption energies of molecular probes (ammonia or pyridine) adsorbed on a catalyst surface and the catalyst acidity is directly proportional. This analogy or relationship as well as the adsorption bond-length of the probes used, were employed to screen the chromium (III) oxide catalyst sites for acidity.

In this study, plots tagged acidity screening maps were employed to screen catalyst sites for acidity based on the adsorption energies (E_{ads}) as shown in Figure 1. The acidity screening map displayed, in terms of adsorption energy on Figure 1 shows the adsorption energy for ammonia on the y-axis and for pyridine on the x-axis. The map shows that as the adsorption energy increases (either increasing downward or leftward of ammonia or pyridine axes respectively), the acidity increases. Moreover, the map shows that there exists a good linear correlation between the ammonia and pyridine adsorption energy due to the its R-squared value of 0.999 obtained for the correlation.

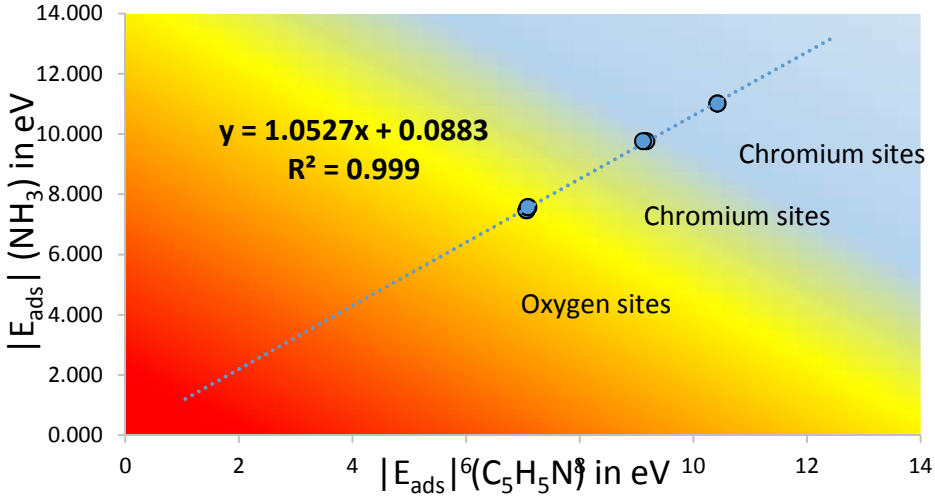

Figure 1: Acidity screening map in terms of adsorption energies.

This implies that there is good agreement between the findings made both when ammonia and pyridine are used as molecular probe. Liu (2017) also give similar report that the resultant outcome from the use of both ammonia and pyridine shows a good correlation.

The adsorption energy map, Figure 1, shows that when ammonia is used as probe, the oxygen sites possess the lowest adsorption energy. When pyridine is used as probe, the chromium sites have the highest adsorption energy, while the oxygen sites have the lowest adsorption energy. The findings suggest that chromium sites is highly acidic compared to other sites due to its high adsorption energy.

Catalyst Reactivity Assessment in Relation to Propane Dehydrogenation

Determination of Chemical Reactivity: The catalyst optimized molecular structure (i.e. Cr_2O_3) have different potential adsorption sites, such as terminal oxygen sites (i.e. O2 and O3), central oxygen site (i.e. O1) and chromium sites (i.e. Cr1 and Cr2). In Table 2, the blue region shows the reactive region or site of the chromium (III) oxide. Table 2 (row 1) confirms that chromium sites have the largest density or surface area on the map. This finding derived from the use of the Fukui frontier electronic molecular orbital theory (HOMO-LUMO approach) suggests that the chromium sites are highly acidic, which agrees with the findings shown on the acidity screening maps earlier discussed.

Propane Adsorption and Dissociation on Chromium (III) oxide Catalyst: The results for the adsorption of propane on the Cr_2O_3 catalyst sites are presented in Figure 2. The results show that chromium sites have lower transition state energy compared to the oxygen sites.

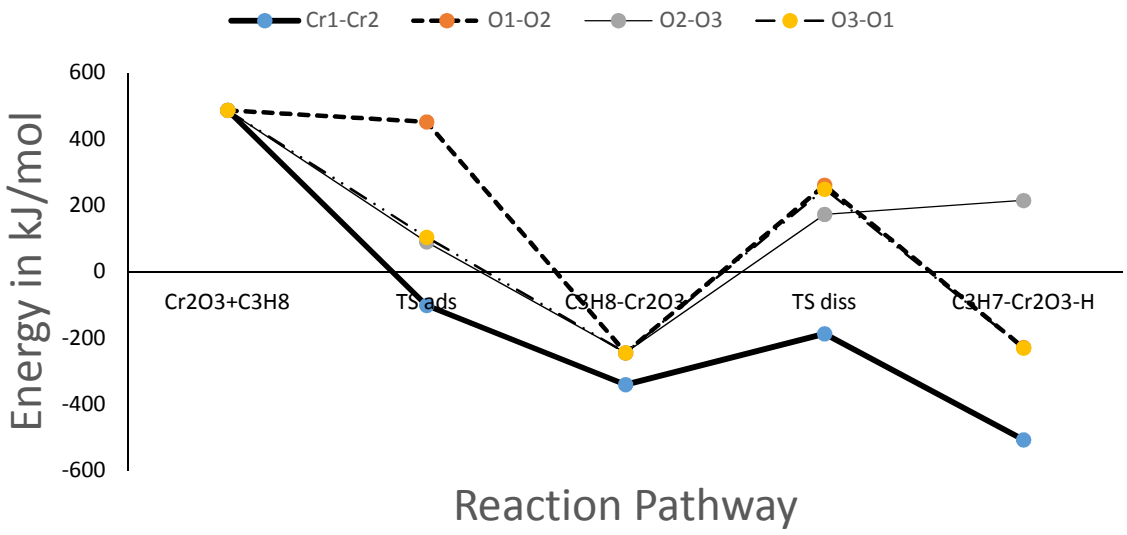

Figure 2: Potential energy surface for propane adsorption and dissociation over different catalyst sites

The activation energies of the oxygen sites were greater than that of the chromium sites as shown on Table 5. This implies that the chromium site will be ready to adsorb the propane due to its high-level of site acidity and lower activation energy compared to the oxygen sites.

Table 5: Activation energies for propane adsorption and dissociation on different catalyst sites

Label	Cr1-Cr2	O1-O2	O2-O3	O3-O1
Ea (Adsorption) in kJ/mol	-588.49	-34.93	-396.68	-382.75
Ea (Dissociation) in kJ/mol	153.36	505.79	417.59	493.51
Adsorption Energy in kJ/mol	-827.38	-731.54	-731.45	-731.45

The nature of activation complexes for the adsorptions at both oxygen and chromium sites show that the step is barrier-less due to their negative activation energies recorded unlike that obtained for propane dissociation. The absolute adsorption energies across the different oxygen sites were found to have the same value (731 kJ/mol), while that obtained for chromium sites was 834 kJ/mol. The values suggest that there is a strong interaction between the catalyst and the propane at the sites, since the values are greater than 100 kJ/mol, which is the minimum value to qualify an interaction as being strong, according to the work of Klaus (2012). The lower absolute adsorption energy across the chromium sites implies that chromium sites will be the most active site to promote the propane adsorption, since it requires lower activation energy or transition state energy.

Table 5 shows the different activation energies for the dissociation steps on catalyst sites on which propane is dissociated into propyl and hydrogen atom. The table shows that chromium sites have the lowest activation energy, while oxygen sites have the highest transition state energy and highest activation energy. This identifies chromium site to be the valid paths which possess high acidity and promote high reactivity of propane over Cr_2O_3 catalyst.

CONCLUSIONS

In this study, the different sites on the chromium (III) oxide were evaluated for acidity and reactivity using the adsorption energies (E). Pyridine and ammonia were used as molecular probes for the evaluation of catalyst sites acidity. The study shows that the bonding strength between the probes and the chromium sites are stronger than that between the probes and the oxygen sites, due to the lower activation energy. The study also suggests that the chromium sites are highly acidic compared to the oxygen sites, as evident by the high adsorption energy and shorter energy barrier or activation complex.

The activation energy of the oxygen sites, which was found to be greater than that of the chromium sites, implies that chromium sites will be the more active site to promote the propane adsorption. The study also shows that for the dissociation of propane into propyl and hydrogen atom, the chromium sites have the least transition state energy and activation energy, and the chromium sites will favour the promotion of propylene production from propane since the oxygen sites on the chromium (III) oxide catalyst have low propane adsorption energy. Thus, this study gives a better insight of the acidity and reactivity of the chromium (III) oxide catalyst for propylene production. This was done through the identification of chromium as the most active, acidic sites and key player in the promotion of propane dehydrogenation into propylene.

REFERENCES

Benco, L., Bucko, T., and Hafner, J. (2011). Dehydrogenation of propane over ZnMOR. Static and dynamic reaction energy diagram. *Journal of catalysis*, 277(1), 104-116.

Bendjeddou, A., Abbaz, T., Gouasmia, A.K., and Villemin, D. (2016). Molecular structure, HOMO-LUMO, MEP and Fukui Functinoal Analysis of Some TTF-donor Substituted Molecules Using DFT (B3LYP) Calculations, *International Research Journal of Pure & Applied Chemistry*, 12(1):1-9.

Biloen, P., Dautzenberg, F.M., and Sachtler, W.M.H. (1977). Catalytic dehydrogenation of propane to propene over platinum and platinum-gold alloys. *Journal of Catalysis*, 50(1), 77-86.

Budavari, S. (1996). *8034 Propylene*. The Merck Index, Twelfth Edition. New Jersey: Merck & Co. pp. 1348–1349.

Fukui, K. (1982). Role of frontier orbitals in chemical reactions. *Science*, 218(4574): 747-754.

Gece, G. (2008). The use of quantum chemical methods in corrosion inhibition studies, *Corrosion Science*, 50(11) 2981-2992.

Gibbs, G.V., Hill, F.C., Boisen, M.B., and Downs, R.T. (1998). Power law relationship between bond length, bond strength and electron density distributions, *Phys. Chem. Mineral*, 25:585-590.

Klaus, C. (2012). Thermodynamics and kinetics of adsorption. *IMPRS-Lecture Series*.

Lauri, N. and Karoliina, H. (2013). Selectivity in Propene Dehydrogenation on Pt and Pt3Sn Surfaces from First Principles, *ACS Catalysis*, 3: 3026−3030.

Li, H., Yue, Y., Miao, C., Xie, Z., Hua, W., and Gao, Z. (2007). Dehydrogenation of ethylbenzene and propane over Ga_2O_3–ZrO_2 catalysts in the presence of CO_2. *Catalysis Communications*, 8(9), 1317-1322.

Liu, C. (2017). Theory of acidity and reactivity in zeolite catalysis Eindhoven: Technische Universiteit Eindhoven, p.40-45.

Maija, H., Jonas, B. and Mats, P., (2012). Computational study of the adsorption and dissociation of phenol on Pt and Rh surfaces, *Physical Chemistry, Chemical Physics - PCCP*, 16(14): 5849-5854.

Maldonado, F. and Stashans, A. (2016). DFT modelling of benzoyl peroxide adsorption on α-Cr_2O_3 (0001) surface, *Surface Review and Letters*, 23(5): 1650037.

Martin, K., Bernhard, M. and Hermann, S. (2000). Breakdown of Bond Length – Bond Strength Correlation: A Case Study, *Angew. Chem. Int. Ed.*, 39(24): 4607-4608.

Ming, L.Y., Yi, A.Z., Xing, G.Z., Zhi, J.S., and De, C. (2012). First-Principles Calculations of Propane Dehydrogenation over PtSn Catalysts, *ACS Catalysis*, 2(6): 1247–1258.

Ming-Lei, Y., Yi-An, Z., Chen, F., Zhi-Jun, S., De, C. and Xing-Gui, Z. (2011). DFT study of propane dehydrogenation on Pt catalyst: effects of step sites, *Physical Chemistry, Chemical Phys*ics, 13: 3257–3267.

Ren, Y., Zhang, F., Hua, W., Yue, Y., and Gao, Z. (2009). ZnO supported on high silica HZSM-5 as new catalysts for dehydrogenation of propane to propene in the presence of CO_2. *Catalysis Today*, *148*(3-4), 316-322.

Stephanie, S., Maarten, K.S., Vladimir, V.G., Evgeniy, A.R., Marie-Françoise, R., and Guy, B.M. (2017). The Positive Role of Hydrogen on the Dehydrogenation of Propane on Pt (111), *ACS Catalysis*, 7 (11): 7495–7508.

Timothy, H., (2015). *Computational study of the catalytic dehydrogenation of propane on Pt and Pt_3Ga catalysts*, Master of Science in Chemical Engineering Thesis, Department of Chemical Engineering and Technical Chemistry, Universiteit Gent.

Warren, H. and Sean, O. (2017). *Spartan 16 for Windows, Macintosh and Linux: User Guide and Tutorial*, CA: Wavefunction, USA, pp. 435-518.

Yan, L., Zhen, H.L., Jing, L., and Kang-Nian, F. (2008). Periodic Density Functional Theory Study of Propane Dehydrogenation over Perfect Ga_2O_3 (100) Surface, *J. Phys. Chem. C*, 2008, 112 (51): 20382–20392.